Accepted Manuscript

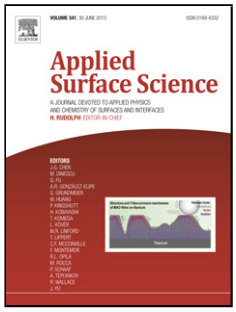

Title: First-principles atomistic Wulff constructions for an equilibrium rutile TiO_2 shape modeling

Authors: Fengzhou Jiang, Lei Yang, Dali Zhou, Gang He, Jiabei Zhou, Fanhou Wang, Zhi-Gang Chen

PII: S0169-4332(17)33637-1
DOI: https://doi.org/10.1016/j.apsusc.2017.12.050
Reference: APSUSC 37920

To appear in: *APSUSC*

Received date: 8-8-2017
Revised date: 7-11-2017
Accepted date: 6-12-2017

Please cite this article as: Jiang F, Yang L, Zhou D, He G, Zhou J, Wang F, Chen Z-G, First-principles atomistic Wulff constructions for an equilibrium rutile TiO_2 shape modeling, *Applied Surface Science* (2010), https://doi.org/10.1016/j.apsusc.2017.12.050

First-principles atomistic Wulff constructions for an equilibrium rutile TiO_2 shape modeling

Fengzhou Jiang[a], Lei Yang[a,f], Dali Zhou[a,*], Gang He[b,*], Jiabei Zhou[c], Fanhou Wang[d], and Zhi-Gang Chen[e,f]

[a]College of Materials Science and Engineering, Sichuan University, Chengdu, 610064, Sichuan, China.

[b]College of computer, Southwest University of Science and Technology, Mianyang, 621010, Sichuan, China.

[c]College of Chemistry, Sichuan University, Chengdu, 610064, Sichuan, China.

[d]Computational Physics Key Laboratory of Sichuan Province, Yibin University, Yibin 640000, PR China.

[e]Centre for Future Materials, University of Southern Queensland, Springfield, QLD 4300, Australia.

[f]Materials Engineering, the University of Queensland, Brisbane, QLD 4072, Australia.

GRAPHICAL ABSTRACT

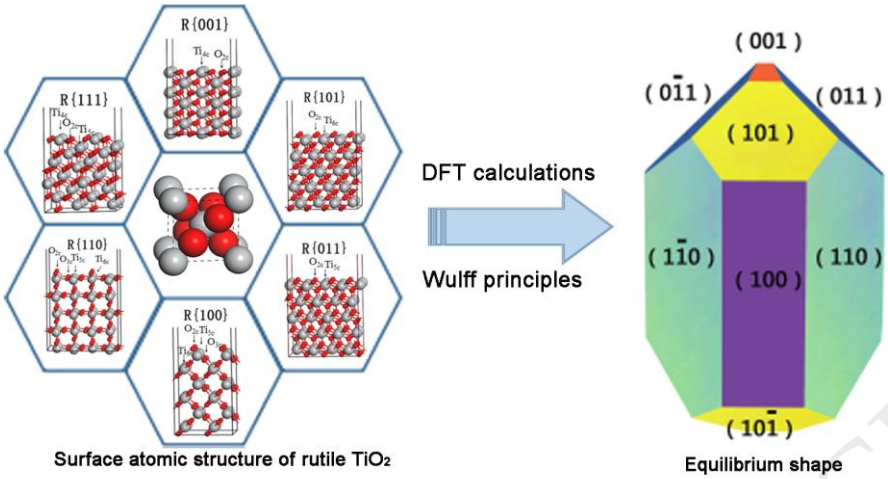

Highlight

- Six low-index surface atomic structures were completely built.
- Surface energies were calculated via first-principles density functional theory (DFT).
- An equilibrium rutile TiO_2 model was constructed based on Wullf principles.
- The established model is in the consistence with typical morphology of fully-developed rutile TiO_2 particles.

Abstract

Identifying the exposed surfaces of rutile TiO_2 crystal is crucial for its industry application and surface engineering. In this study, the shape of the rutile TiO_2 was constructed by applying equilibrium thermodynamics of TiO_2 crystals via first-principles density functional theory (DFT) and Wulff principles. From the DFT calculations, the surface energies of six low-index stoichiometric facets of TiO_2 are determined after the calibrations of crystal structure. And then, combined surface energy calculations and Wulff principles, a geometric model of equilibrium rutile TiO_2 is built up, which is coherent with the typical morphology of fully-developed equilibrium TiO_2 crystal. This study provides fundamental theoretical guidance for the surface analysis and surface modification of the rutile TiO_2-based materials from experimental research to industry manufacturing.

Keywords: Rutile TiO_2, DFT calculations, Wulff principle, equilibrium model.

1. Introduction

Titanium dioxide (TiO_2) is well-known as primary white pigment and one of the most important fine chemical materials [1, 2], which has extensive industry applications, including photocatalytic degradations [3], sensors [4], cosmetics [5], coating [6] and photovoltaics [7, 8]. The performance of the TiO_2 is highly affected by its crystalline phase (rutile, brookite or anatase), particle size, surface energy state and morphology [9, 10]. In general, nano-sized rutile TiO_2 is the most important industrial TiO_2-based material and has drawn much attentions due to its unique properties [11-13]. For stoichiometric rutile TiO_2, its {110} plane (R{110}) has been proved to have the lowest energy and to be energetically the most stable planes in both experimental and theoretical works [14, 15]. Therefore, {110} facets are usually the main exposed surfaces of rutile TiO_2. From first-principles calculations, extensive investigations [8, 14-18] show that the oxygen vacancies on the surface significantly affect the absorption and reaction on R{110}. Hussain *et al.* [17] constructed a model of R{110} interacting with water, in which a solid liquid interface between TiO_2 and water can be expected because all five coordination Ti sites were occupied by half a monolayer of terminal hydroxyls. This finding reveals that the surface absorption behavior of R{110} facets in rutile TiO_2 is crucial to guide the practical industry applications.

Meanwhile, researchers have also paid much attention on other high-energy planes of the rutile TiO_2 due to their high reactivity as well as their merits in industry applications. Rutile TiO_2 rods with exposed {111} facets show high photocatalytic

activity [19, 20]. Dumbbell-shaped rutile TiO_2 particles with exposed {001} facets were successfully fabricated by using different counterions and display improved lithium storage properties [10]. Ahmed *et al.* [21] produced rutile TiO_2 single crystal with {011} facets by wet chemical preparation, presenting a non-ultra-high vacuum recipe for preparing the prototypical metal oxide surface. Ramamoorthy *et al.* [22] also investigated the shape of rutile TiO_2 after the surface energy calculations of only four main facets including R{110}, R{100}, R{101} and R{011}. However, systematic research that involves all the possible exposed facets and the equilibrium rutile TiO_2 shape is still urgently demanded for guiding the surface modification or absorption of TiO_2 in industry applications [23].

In this work, we construct a comprehensive low-index stoichiometric facets model based on rutile TiO_2 geometry optimization through first-principle density functional theory (DFT) [24]. According to the surface energy calculations, a geometric model of equilibrium rutile TiO_2 particle with five low-index exposed facets was constructed by the Wulff grain growth principles. The model shows a good agreement with the fully-developed raw TiO_2 particles that obtained in experiment, which will provide theoretical guidance for surface energy analysis and surface modifications of rutile TiO_2-based materials [25].

2. Calculations and Analysis

The calculations were performed using the DFT and Cambridge Serial Total Energy Package (CASTEP) codes, employing the ultrasoft pseudopotential expanded in a

planewave basis [26]. Exchange and correlation effects were treated by the revised Perdew-Burke-Ernzerhof (PBE) function [27] within the generalized gradient approximation (GGA) [28]. The calculation has been performed in an iterative process, in which the coordinates of the atoms are adjusted so that the total energy of the structure is minimized [21]. Structural relaxation was carried out using a Broyden-Fletcher-Glodfarb-Shanno (BFGS) algorithm [29] with full relaxation taken to be when none of the forces exceeded 0.03 eV/Å and none of the stresses exceeded 1.0E-05 eV/atom. The stress on the atom was less than 0.05 GPa and the displacement of the atom was less than 0.001 Å. We used an energy cutoff 420 eV and a k-points grid of Monkhorst-Pack [30] 4×4×1 in the Brillouin zone. The third number of k-points is always small, 1 or 2, just for ignoring the periodic of the z axis. In three-dimensional (3D) periodic geometry, a slab of atoms separated by a 10 Å thickness vacuum layer was used to model the surface. To get an accurate result, parameter settings have been extensively tested and fully meet the requirements of calculation convergence.

2.1 Crystal structure of TiO_2 and analysis

The space group of rutile TiO_2 is P42 /mnm with lattice parameters of $a = b = 4.59$ Å, $c = 2.96$ Å, and belongs to tetragonal crystal system. Ti atoms coordinate in (0，0，0) and (1/2, 1/2, 1/2) positions while oxygen atoms in ±(u, u, 0) and ±(u+1/2, 1/2-u, 1/2) positions, respectively. The model of TiO_2 crystal was constructed using Materials Studio (Accelrys) as shown in Fig. 1(a), in which each unit cell contains

two TiO_2 units.

There are one Ti atom in the center of each cell and eight Ti in the corners which contribute overall 2 Ti atoms to each cell. Each O atom is threefold coordinated to Ti atom with different Ti-O bonds' lengths. The lengths of Ti-O bonds are 1.98 Å and 1.95 Å. Every threefold coordinated oxygen atoms have one long and two short Ti-O bonds; And two apical Ti-O bonds are longer than the four equatorial Ti-O bonds.

Geometry optimization has been realized for the established TiO_2 crystal structure to reach the minimum system energy. The lengths of long and short Ti-O bonds were adjusted to 2.01Å and 1.96Å, respectively, which caused a slightly expansion of the unit cell. The crystal parameters of the geometry optimization are shown in Table 1. Comparing to the experimental results and reported theoretical calculations (marked as 1 and 2 in Table 1), the optimized parameters show good reliability with a low relative error of ~ 2%. In all the subsequent calculations, we used the optimized lattice constants for the input parameters.

Table 1. Geometry optimization result of TiO_2

	a (Å)	*b* (Å)	*c* (Å)	U
unrelaxed	4.594	4.594	2.959	0.3048
Relaxed	4.664	4.664	2.968	0.3054
theoretical 1[31]	4.536	4.536	2.914	0.304
theoretical 2[32]	4.653	4.653	2.975	0.306
experimental[33]	4.623	4.623	2.984	0.306

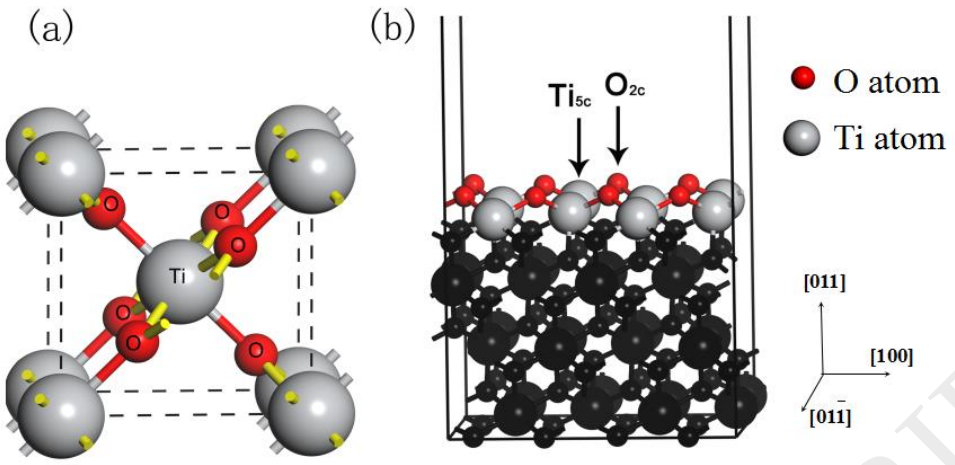

Fig. 1. (a) Rutile TiO_2 crystal structure. (b) Model of R{011} plane, the black atoms are constrained Ti and O atoms for relaxation.

2.2 Supercell modeling and surface energy calculation

The surface energy of each facet is calculated from the total energy of a (2×1) supercell of six surface orientations as follows [34, 35]:

$$E_{surf} = (E_{slab} - N \cdot E_{bulk}) / (m \cdot S) \quad (1)$$

where E_{surf} is the surface energy; E_{bulk} is the total energy of a bulk TiO_2; E_{slab} is the total energy of the given supercell, containing N TiO_2 units; And m represents the number of surfaces for relaxation. The calculation of surface energy is based on structure optimization of the supercell with a superficial area of S.

We built a four-layer slab of {011} orientation. The surface has two kinds of exposed atoms including fivefold coordination titanium atoms (Ti_{5c}) and twofold coordination oxygen atoms (O_{2c}), connecting to Ti_{5c}. Herein, m is 1 as we relaxed the surface atoms while the under-layer atoms were constrained, as colored in black..Fig.

2(a) is the typical structure of R{011} after relaxation. Since surface Ti and O atoms both slightly moved and the O atoms has a smaller moving distance than Ti atoms, the bond length between surface O and Ti atoms (named Ti-1– O-1, Ti-3– O-1) is slightly smaller than that of bulk phase. Besides, Ti atoms also have a tiny horizontal movement which leads to a closer distance between Ti and O atoms.

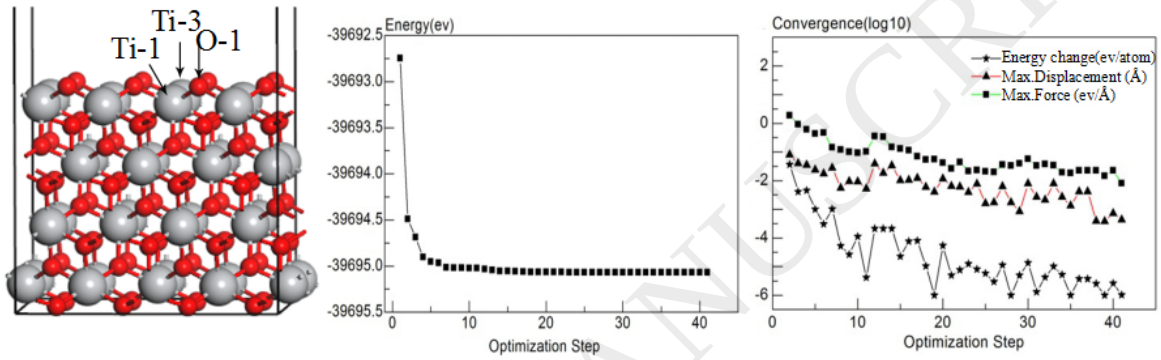

(a) (b) (c)

Fig. 2. (a) The changed structure of R{011}. (b) Energy evolution curve of R{011} relaxing. (c) Convergence curve of R{011} relaxing.

The orbits of O-$2s^2 2p^4$ and Ti-$3s^2 3p^6 3d^2 4s^2$ were used in DFT calculations. The used lattice parameters are a = 9.12 Å, b = 5.487 Å, c = 28.94 Å, $\alpha = \beta = \gamma = 90°$. After relaxation, E_{slab} = -39695.07 eV can be determined. According to equation 1, the surface energy of {011} facet can be calculated as 1.11 J/m^2. In Fig. 2, (b) and (c) show the energy convergence curve and self-consistent convergence curve during calculation. As can be seen, the energy of the system drops rapidly in the first five steps of calculation and then stabilizes gradually. The convergence curve indicates that the system can well reach to a stable state with minimum energy.

Then we established other five low-index facet models, shown in Fig. 3. According to the report [33], the pure rutile TiO_2 {110} surfaces have two different Ti atoms of Ti_{5c} and six-fold coordination titanium atoms (Ti_{6c}). The oxygen atoms bonding with two Ti_{6c} are O_{2c} and the ones bonding with Ti_{5c} are the unsaturated threefold coordination oxygen (O_{3c}). R{100} has the same atoms as R{110} on surface. For R{101}, there are two-type atoms of Ti_{5c} and O_{2c} on surface. Also, there are two-type atoms of Ti_{4c} and O_{2c} on the surface of R{001} [36]. R{111} has the atoms of Ti_{5c}, Ti_{4c} and O_{2c} on its surface. The four coordination Ti atoms contain high unsaturated valence, which leads to acidity. Building these six low-index surface structures is the crucial first step to model complex adsorption [8] and mixture processes [18] in each surface.

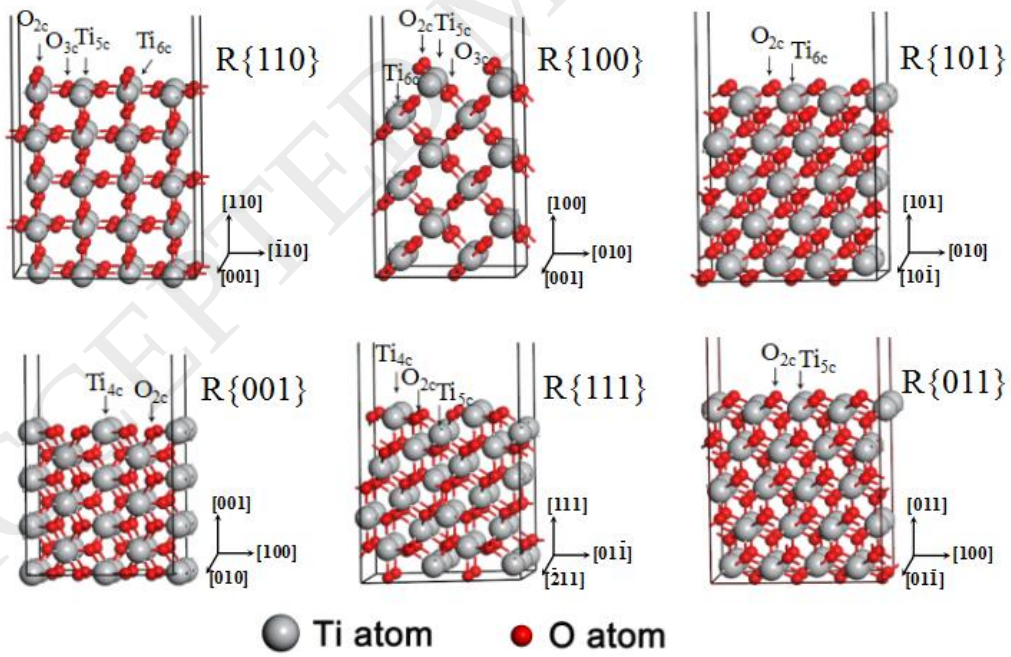

Fig. 3. Models of R{110}, R{100}, R{101}, R{001}, R{111} and R{011} planes.

After modeling each surface structure, we constrained under-layer atoms for relaxation. The changes of surface atoms before and after the relaxation are shown in Table 2. The coordination atoms and charge distribution changed during relaxation, which results in the surface-layer has a displacement. The change of Ti atoms in the Z direction of the slab is greater than the O atoms, which is mainly due to their different electronic orbits, namely Ti-$3s^2 3p^6 3d^2 4s^2$ and O-$2s^2 2p^4$, respectively. The surface atoms of R{110} have larger displacement than the atoms of other surfaces. In R{001} and R{111} surfaces, Ti_{4c} atoms present greater displacement than Ti_{5c} and Ti_{6c} atoms in other surfaces due to the high unsaturated valence. The change of atomic parameters on the surface during the relaxation can significantly affect the surface energy calculation.

Table 2. Displacement of surface atoms along Z-axis.

facet	surface atoms	ΔZ (Å)	ΔZ Ref. (Å)
R{110}	Ti(6c)	0.198	0.23 [35]
	Ti(5c)	-0.153	-0.11 [35]
	O(2c)	-0.009	-0.02 [35]
	O(3c)	0.195	0.18 [35]
R{101}	Ti(5c)	-0.059	
	O(2c)	-0.055	-0.1 [37]
R{001}	Ti(4c)	-0.168	
	O(2c)	-0.06	-0.09 [37]
R{100}	Ti(5c)	-0.088	
	O(2c)	-0.011	-0.11 [37]

R{011}	Ti(5c)	0.094
	O(2c)	0.016
R{111}	Ti(4c)	-0.301
	O(2c)	-0.097

After that, we calculated the surface energy of six facets using the Equation 1 and the results are listed in Table 3. As can be seen, R{110} has the lowest surface energy [14], while R{001} and R{111} have the highest surface energy. Such information is crucial to guide the research on surface modification or industry manufacturing [23].

Table 3. Surface energy of the six rutile facets.

	R{110}	R{101}	R{100}	R{001}	R{011}	R{111}
E_{slab} (eV)	-14886.56	-14884.88	-49622.64	-27291.32	-39695.07	-59542.39
E_{bulk} (eV)	-4962.78	-4962.78	-4962.78	-4962.78	-4962.78	-4962.78
N	3	3	10	5.5	12	12
m*S (Å^2)	38.45	50.21	108.75	42.21	103.13	117.06
E_{surf} (J/m^2)	0.74	1.11	0.76	1.51	1.11	1.51
E_{surf} (Ref.) (J/m^2)	0.73 [34]	1.39 [34]	0.83 [22]	1.65 [22]	1.50 [35]	1.46 [38]

3. Modeling an equilibrium TiO_2 shape

3.1 Wulff grain growth principles

Wulff principles [39] are widely used in the grain growth with the request that the terminal geometrical shape of crystal grain has a minimum surface energy, as shown

in Equation 2.

$$\sum_{i=1}^{\infty} S_i \gamma_i = \text{Min} \quad (2)$$

$$\gamma_1 : \gamma_2 : \gamma_3 \ldots\ldots = n_1 : n_2 : n_3 \ldots\ldots \quad (3)$$

Where S_i is the area of the facet belongs to No. i; γ_i is the surface energy of the facet belongs to No. i and n_i is the length of normal from crystallization center of the facet belongs to No. i.

When we construct a model shape, we follow Wulff drawing principle to determine the exposed surface, as shown in Equation 3. The ratio of normal length from crystallization center equals to the ratio of surface energy. Therefore, the facets with low energy are preferred to be exposed during the growth. The high energy facets have always been covered by other adjacent facets during process of the growth of the crystal due to the faster growth rate in the normal direction [39]. The facets with lower energy are always the low-index facets, which leads to a result that the final exposed surface should be low-index facets.

3.2 Modeling

According to the calculated surface energy of the rutile TiO_2 in Table 3, we built a model of equilibrium TiO_2 crystal structure in 3D Auto CAD drawing software (Autodesk) using Wulff principles. Each facet has a miller index corresponding to a space position as shown in Fig. 4(a). In Fig. 4(a), there are five different facets on the exposed surface while R{111} disappeared, which is more comprehensive compared

to the model of TiO_2 built by Ramamoorthy *et al.* (Fig. 4(b)), In their study, only four main facets of rutile TiO_2 was calculated, including R{110}, R{100}, R{101} and R{011}.

The energies of R{111} and R{001} are both 1.51 J/m^2, which are the highest in six low-index facets. Such high energy leads to the fastest growth rate along the normal direction during equilibrium growth. In rutile TiO_2, R{111} planes are not exposed because they are covered by adjacent facets that have slower growth rate, while the exposed surface area of R{001} is a small rectangle adjacent with R{011} and R{101}. The exposed surface area of R{011} and R{101} are both hexagonal shape, which significantly prevents the disappearance of R{001}. As a result, the model with large exposed areas of R{110}, R{011} and R{101} but a very small exposed area of R{001} shows a slim rod-like shape, which is different from the previous model developed by Ramamoorthy *et al* [22]. Our model has been established reliably with significant precision of six low-index facets that can be used as an initial model for further reaction mechanism of complex adsorption and mixture processes.

To verify our built model, we further analyze the morphology of industrial grade rutile TiO_2 and the typical morphology is shown in Fig. 4(c). As can be seen, one facet particle is observed and can be indexed by the miller index (*hkl*) for each crystal facet, shown in Fig. 4(d). The shape and exposed surfaces are consistent with the equilibrium TiO_2 shape modeled above, which verifies our accuracy of the DFT calculation and Wulff principle modeling.

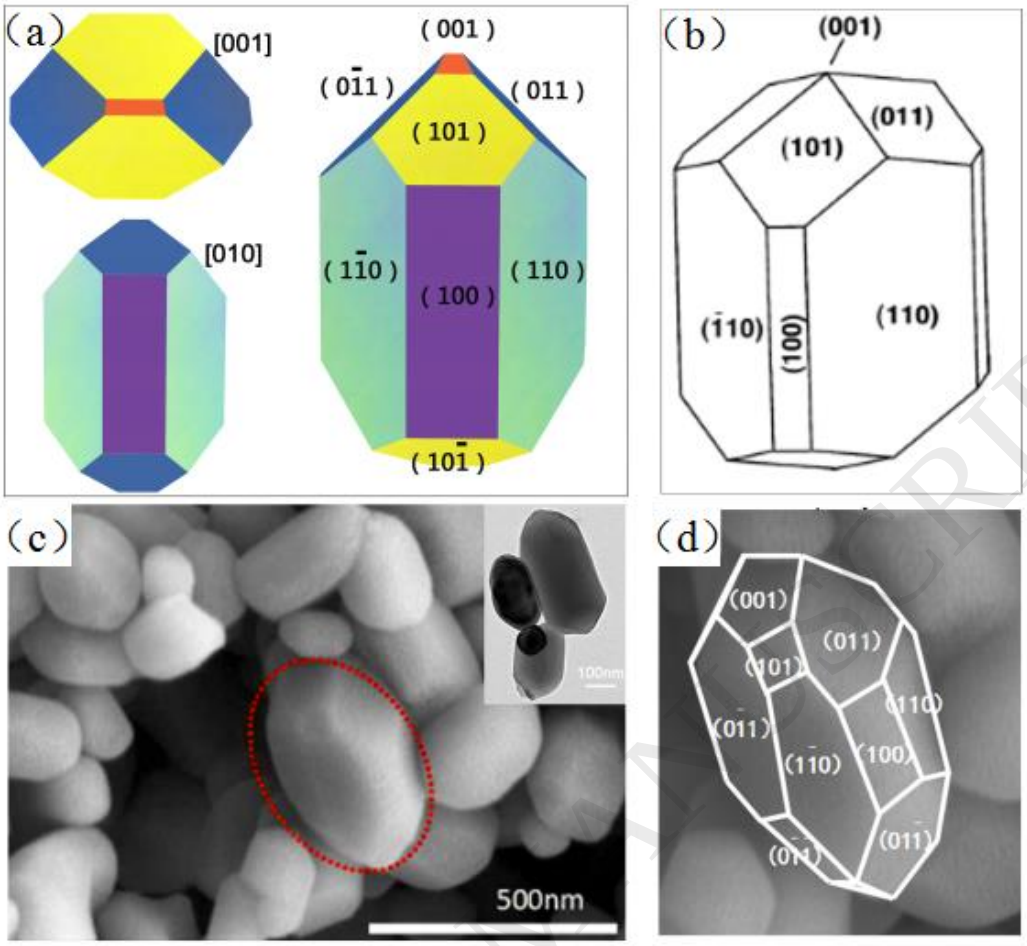

Fig. 4. (a) The equilibrium model of TiO_2 crystal (the left part views from [001] and [010] respectively, the right part is the bulk to show main exposed facets.). (b) TiO_2 crystal modeled by Ramamoorthy [22] for comparison. (c) SEM image of rutile TiO_2 particles, inset a typical TEM. (d) High magnification SEM image of the marked particle in (c) shows facets consistent with our modeling result.

4、Conclusion

In summary, an equilibrium rutile TiO_2 model with five low-index exposed facets was constructed using first-principles DFT calculations and Wulff principles.

Moreover, the R{110} has the lowest energy while R{001} and R {111} are the highest energy, leading to a high reactivity. The established model is in the consistence with typical morphology of fully-developed rutile TiO_2 particles, which suggests that this study is more comprehensive and accurate compared to previously theoretical modeling results. The developed knowledge of exposed surfaces could provide theoretical guidance for surface analysis in industry application of TiO_2.

References

[1] D. Ulrike, The surface science of titanium dioxide. Surf. Sci. Rep. 48 (2003) 53-229.

[2] A. R. Padua, TiO_2 conference: industry takes stock, Paint Ink. Int. 12 (1999) 24–27.

[3] J. Labille, J. Feng, C. Botta, D. Borschneck, M. Sammut, M. Cabie, M. Auffan, J. Rose, J. Y. Bottero, Aging of TiO_2 nanocomposites used in sunscreen. Dispersion and fate of the degradation products in aqueous environment, Environ. Pollut. 158 (2010) 3482–3489.

[4] X. Hu, G. Li, J.C. Yu, Design, fabrication, and modification of nanostructured semiconductor materials for environmental and energy applications, Langmuir 26 (2009) 3031-3039.

[5] M. Buchalska, G. Kras, M. Oszajca, W. Lasocha, W. Macyk, Singlet oxygen generation in the presence of titanium dioxide materials used as sunscreens in suntan lotions, J. Photochem. Photobiol. A: Chem. 213 (2010) 158-163.

[6] J. J. Yuan, S. X. Zhou, L.M. Wu, Y. Bo, Organic pigment particles coated with titania via Sol-Gel process, J. Phys. Chem. B. 110 (2006) 388-394.

[7] K. S. Venkatesh, S. R. Krishnamoorthi, N. S. Palani, V. Thirumal, P. J. Sujin, F. M. Wang, R. Ilangovan, Facile one step synthesis of novel TiO_2 nanocoral by sol-gel method using aloevera plant extract, Indian J. Phys. 89 (2015) 445-452.

[8] H. Xu, S.Y. Tong, Interaction of O_2 with reduced rutile TiO_2 (110) surface, Surf. Sci. 610 (2013) 33-41.

[9] J. Pan, G. Liu, G. Q. Lu, H. M. Cheng, On the true photoreactivity order of {001}, {010}, and {101} facets of anatase TiO_2 Crystals, Angew. Chem. (2011) 2133-2137.

[10] Z. Hong, Y. Xu, Y. Liu, M. Wei, Unique ordered TiO_2 superstructures with tunable morphology and crystalline phase for improved lithium storage properties, Chem. A (2012) 00515.

[11] M. A. Henderson, A surface science perspective on TiO_2 photocatalysis, Surf. Sci. Rep. 66 (2011) 185-297.

[12] J. Pan, X. Wu, L. Wang, G. Liu, G. Q. Lu, H. M. Cheng, Synthesis of anatase TiO_2 rods with dominant reactive {010} facets for the photoreduction of CO_2 to CH_4 and use in dye-sensitized solar cells, Chem. Commun. 47 (2011) 8361-8363.

[13] G. Liu, L. C. Yin, J. Wang, P. Niu, C. Zhen, Y. Xie, H. M. Cheng, A red anatase TiO_2 photocatalyst for solar energy conversion, Energy Environ. Sci. 5 (2012) 9603-9610.

[14] K. Matsunaga, Y. Tanaka, K. Toyoura, K. Nakamura, A. Ikuhara, Y. Shibata, Naoya, Existence of basal oxygen vacancies on the rutile TiO_2 (110) surface, Phys. Rev. B 90 (2014) 195303.

[15] S. D. Elliott, S. P. Bates, Assignment of the (1×2) surface of rutile TiO_2 (110) from first principles, Phys. Rev. B 67 (2003) 035421.

[16] Z. L. Zeng, First-Principles study on the structural and electronic properties of N atoms doped-rutile TiO_2 of oxygen vacancies, Adv. in Mater. Sci. and Eng. (2015) 670243.

[17] H. Hussain, G. Tocci, T. Woolcot, X.Torrelles, C. L. Pang, D. S. Humphrey, C. M. Yim, D. C. Grinter, G. C. abailh, O. Bikondoa, R. Lindsay, J. Zegenhagen, A. Michaelides, G. Thornton, Structure of a model TiO_2 photocatalytic interface, Nature Mater. (2016) 461-466.

[18] X. Li, X. F. Sun, X. L. Xu, W. M. Liu, H. G. Peng, X. Z. Fang, H. M. Wang, X. Wang, CO oxidation on PdO catalysts with perfect and defective rutile-TiO_2 as supports: Elucidating the role of oxygen vacancy in support by DFT calculations, Appl. Surf. Sci. 401 (2017) 49-56.

[19] J. Zhang, P. L. Liu, Z. D. Lu, G. L. Xu, X. Y. Wang, L. S. Qian, H. B. Wang, E. Zhang, J. H. Xi, Z. G. Ji, One-step synthesis of rutile nano-TiO_2 with exposed {111} facets for high photocatalytic activity, J. Alloy. Compd. 632 (2015) 133–

139.

[20] K. Kakiuchi, E. J. Hosono, H. Imai, T. Kimura, S. Fujihara, {111}-faceting of low-temperature processed rutile TiO_2 rods, J. Cryst. Growth 293 (2006) 541-545.

[21] M. H. M. Ahmed, F. P. Lydiatt, D. Chekulaev, P. L. Wincott, D. J. Vaughan, J. H. Jang, S. Baldelli, A. G. Thomas, W. S. Walters, R. Lindsay, Wet chemically prepared rutile TiO_2 (110) and TiO_2 (011): Substrate preparation for surface studies under non-UHV conditions, Surf. Sci. 630 (2014) 41-45.

[22] M. Ramamoorthy, D. Vanderbilt, R. K. Smith, First-principles calculations of the energetics of stoichiometric TiO2 surfaces, Phys. Rev. B 49 (1994) 16721.

[23] Z. Y. Zhao, Single water molecule adsorption and decomposition on the low-index stoichiometric rutile TiO_2 surfaces, J. Phys. Chem. C 118 (2014) 4287-4295.

[24] V. Milman, K. Refsonb, S. J. Clark, C. J. Pickard, J. R. Yates, S. P. Gao, P. J. Hasnip, M. I. J. Probert, A. Perlov, M. D. Segall, Electron and vibrational spectroscopies using DFT, plane waves and pseudopotentials: CASTEP implementation, J. Mol. Struc.-Theochem 954 (2010) 22-35.

[25] J. Zhang, W. Fu, J. Xi, H. He, S. C. Zhao, H. W. Lu, Z. G. Ji, N-doped rutile TiO_2 nano-rods show tunable photocatalytic selectivity, J. Alloy. Compd. 575 (2013) 40-47.

[26] S. J. Clark, M. D. Segall, C. J. Pickard, P. J. Hasnip, M. I. J. Probert, K. Refson , M. C. Payne, First principles methods using CASTEP, Z. Kristalllogr-Crystalline Mater. 220 (2005) 567-570.

[27] V. Pallassana, M. Neurock, L. B. Hansen, B. Hammer, J. K. Nørskov, Theoretical analysis of hydrogen chemisorption on Pd (111), Re (0001) and Pd ML/Re (0001), Re ML/Pd (111) pseudomorphic overlayers, Phys. Rev. B 59 (1999) 7413.

[28] J. P. Perdew, A. Ruzsinszky, G. I. Csonka, O. A. Vydrov, G. E. Scuseria, L. A. Constantin, X. L. Zhou, B. Kieron, Restoring the density-gradient expansion for exchange in solids and surfaces, Phys. Rev. Lett. 100 (2008) 136406.

[29] B. G. Pfrommer, M. Côté, S. G. Louie, M. L. Cohen, Relaxation of crystals with the quasi-newton method, J. Comput. Phys. 131 (1997) 233-240.

[30] H. J. Monkorst, J. D. Pack, Special points for Brillouin-zone integrations, Phys.

Rev. B 13 (1976) 5188 .

[31] E. Cho, S. Han, H. S.Ahn, K. R. Lee, S. K. Kim, C. S. Hwang, First-principles study of point defects in rutile TiO_2, Phys. Rev. B 73 (2006) 193202.

[32] F. Labat, P. Baranek, C. Adamo, Structural and electronic properties of selected rutile and anatase TiO_2 surfaces: an ab initio investigation, J. Chem. Theory Comput. 4 (2008) 341-352.

[33] F. Lindberg, J. Heinrichs, F. Ericson, P. Thomsen, H. Engqvist, Hydroxylapatite growth on single-crystal rutile substrates, Biomaterials 29 (2008) 3317-3323.

[34] S. Bates, G. Kresse, M. Gillan, A systematic study of the surface energetics and structure of TiO_2 (110) by first-principles calculations. Surf. Sci. 385 (1997) 386-394.

[35] H. Perron, C. Domain, J. Roques, R. Drot, E. Simoni, H. Catalette, Optimisation of accurate rutile TiO_2 (110), (100), (101) and (001) surface models from periodic DFT calculations, Theor. Chem. Acc. 117 (2007) 565-574.

[36] S. Munnix, M. Schmeits, Electronic structure of ideal TiO_2 (110), TiO_2 (001), and TiO_2 (100) surfaces, Phys. Rev. B 30 (1984) 2202.

[37] H. Zhang, X. Liu, Y. Wang, P. Liu, W. Cai, G. Zhu, H. Yang, H. Zhao, Rutile TiO_2 films with 100% exposed pyramid-shaped (111) surface: photoelectron transport properties under UV and visible light irradiation, J. Mater. Chem. A 1 (2013) 2646-2652.

[38] Y. Wang, T. Sun, X. Liu, H. Zhang, P. Liu, H. Yang, X. Yao, H. Zhao, Geometric structure of rutile titanium dioxide (111) surfaces, Phys. Rev. B 90 (2014) 045304.

[39] R. F. Sekerka, Theory of crystal growth morphology, in: G. Müller, J. Métois, P. Rudolph (Eds.), Crystal growth-from fundamentals to technology, Elsevier Science Ltd, 2004, pp. 55-93.